Available online at www.sciencedirect.com
ScienceDirect
Journal of Power Sources 180 (2008) 365–372
JOURNAL OF POWER SOURCES
www.elsevier.com/locate/jpowsour

Separate measurement of current density under the channel and the shoulder in PEM fuel cells

Lin Wang, Hongtan Liu *

Department of Mechanical and Aerospace Engineering, University of Miami, Coral Gables, FL 33146, USA

Received 22 January 2008; accepted 30 January 2008
Available online 16 February 2008

Abstract

In a proton exchange membrane (PEM) fuel cell current density under the shoulder can be very different from that under the gas channel and the knowledge of where the current density is higher is critical in flow field designs in order to optimize fuel cell performance. Yet, up to date this issue has not been resolved. In this study, a novel yet simple approach was adopted to directly measure the current densities under the channel and the shoulder in PEM fuel cells separately. In this approach, the cathode catalyst layer was so designed that either the area under the shoulder or the area under the channel was loaded with catalyst. Such a design guaranteed the currents generated under the shoulder and the channel could be measured separately. Experimental results showed that the current density produced under the channel was lower than that under the shoulder except in the high current density region. To determine the causes of higher current density under the shoulder two additional sets of experiments were conducted. First, a silver mesh was added on the top of the gas diffusion layer (GDL) and the experimental results showed that GDL lateral electrical resistance was not the cause and it had a negligible effect on lateral current density variation. Secondly, the total through-plane electric resistance of the GDL and the catalyst layer under different compressions was measured and the results showed that the difference between the total through-plane electrical resistance under the channel and under the shoulder was large enough to cause the higher current density under the shoulder.

Keywords: Fuel cell; PEM fuel cell; Current distribution; GDL electric resistance

1. Introduction

It is well known that current density is not uniform in a fuel cell and the knowledge of local current density variations is essential in fuel cell design and optimizations. Measurement of local current density can also be used as diagnostic tools for fuel cells operation. To date, various techniques of measuring local current density in a PEM fuel cell have been devised and reported.

Brett et al. [1] measured the current distribution along a single channel using the printed circuit board approach. The current distribution was studied under different polarizations and air-flow rates. The study showed the depletion of reactant along the channel and slow reaction rate at low air-flow rate. Mench et al. [2] also presented a study on current distribution measurement along a serpentine channel. They used a segmented flow field with current-conducting wires. The effect of cathode flow rate on the current along the channel was studied and mass-limited performance was observed. The transient current density was measured, which showed a slow flooding process until the steady state was achieved. The research group of Nguyen has carried out a series of experimental studies on current distributions [3–5]. Firstly a study of measurement of current density and potential distribution along a straight channel was developed and reported [3]. Based on this experimental work, further experiments studying the effects of reactant flow rates, gas stream humidity and cell temperature on the current distribution in a PEM fuel cell were carried out [4,5]. Their results showed that the current distribution was affected by reactant flow rates, gas humidity and cell temperature simultaneously.

Other experiments have been carried out to measure the current distribution in segments. Cleghorn et al. [6] presented a

* Corresponding author at: Department of Mechanical and Aerospace Engineering, University of Miami, PO Box 248294, Coral Gables, FL 33146, USA. Tel.: +1 3052842019; fax: +1 3052842580.
E-mail address: hliu@miami.edu (H. Liu).

0378-7753/$ – see front matter © 2008 Elsevier B.V. All rights reserved.
doi:10.1016/j.jpowsour.2008.01.091

printed circuit board approach of measuring current distribution. The current collector, flow field and electrode were composed of large segments. The currents collected on each segment were measured. The current distribution was studied under different stoichiometric flow of air. Stumper et al. [7] presented three in situ methods of measuring current distribution in large segments. One of them was a partial MEA approach. The local current produced in one part of the catalyst layer was measured by using a MEA with partially loaded catalyst. The second method was a sub-cell approach, in which a few isolated sub-cells were placed in the MEA and currents were collected from the sub-cells respectively. This method has been employed by others [8,9]. The third method was the current mapping technique, which employs a passive resistor network distributed over the entire MEA area. Later Ghosh et al. [10] measured the current distribution of a fuel cell under different operation conditions using the same method. Wieser et al. [11] presented a technique of using magnetic loop array to measure current distribution. The flow field of straight channels was segmented and attached with annular ferrites and Hall sensors. Büchi et al. [12] developed a PEM fuel cell with semi-segmented collector plate to study the water management on current distribution. The semi-segmented plate had a regular flow field on one side and segmented electricity collector on the other side. Sun et al. [13,14] developed a measuring gasket technique to measure current distribution in fuel cells. In the test fuel cell, a measuring gasket with a number of strips was inserted between the flow field plate and the gas diffusion layer. The currents produced in the part of the catalyst layer corresponding to each strip were measured. The effects of gas humidification, cell temperature, reactant flow rate and pressure on current distribution as well as transient effects were studied. Similar work of measuring current distribution in large segments using segmented flow field and segmented gas diffusion layer has been reported [15–20]. Recently Freunberger et al. [21] presented a technique for measuring the current density distribution across the channel and shoulder direction. Unfortunately, this is an indirect technique that requires precise knowledge of all resistance involved, including the contact resistance between the GDL and the collector plate shoulder. Some of the values must be obtained from solving potential equations, Laplace equations, and other values must come from complicated and stringent measuring techniques.

As can be seen from the above, almost all of the studies were focused on measuring local current density distribution either along the gas channels or in segments. There is obvious critical need to measure lateral current density variations in a fuel cell, yet the small dimensions of the channels and shoulders (order of 1 mm) and the difficulty associated with electrically isolation of the shoulder from the channel have primarily prevented progress in this area.

Unable to directly measure the lateral current density distribution, most researchers have resorted to modeling to predict the local current densities. The earlier models neglected electric resistance of the GDL as well as of the catalyst layer and the collector plates and these models predicted that the current density under the shoulder to be always much lower than that under the channel (e.g. [22–25]). For instance, Natarajan and

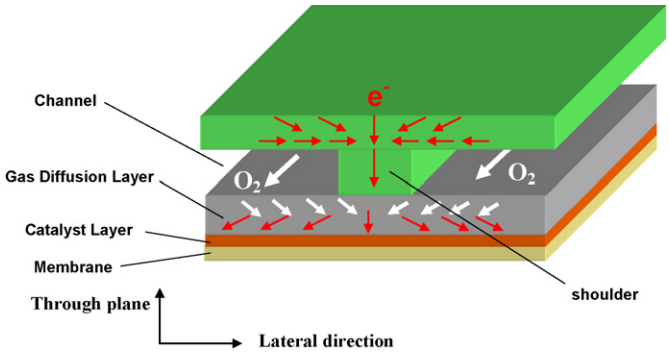

Fig. 1. Schematic of lateral oxygen and electron transports under the channel and shoulder.

Nguyen [25] showed that the current density under the shoulder was essentially zero when the shoulder width is greater than 2 mm.

Some recent modeling work [26–28] took into consideration of the electric resistance of the GDL and these models predicted that the lateral electrical resistance of the GDL has a very significant effect on the lateral current density distribution in a fuel cell. Furthermore, some of the results predicted a higher current density under the shoulder, which is in contrast to all the previous modeling results. To facilitate our discussions, Fig. 1 is used to demonstrate the electron and oxygen transports at the cathode side of a PEM fuel cell. For the reaction occurs under the channel, electrons from the shoulder of the collector plate must transfer laterally through the GDL. The hypotheses was that this additional conduction path would result in a lower overpotential over the channel than that under the shoulder and this difference in local overpotential could cause the local current density to be higher under the shoulder since current density depends on the overpotential exponentially, as shown in the Butler–Volmer equation:

$$j_c = (ai_0^{\mathrm{ref}})_c \frac{c_{O_2}}{c_{O_2}^{\mathrm{ref}}} \left(e^{\frac{\alpha_c^a F}{RT}\eta_c} - e^{-\frac{\alpha_c^c F}{RT}\eta_c}\right) \quad (1)$$

It can be seen from Eq. (1) that the only difference for the areas under the channel and the shoulder are local oxygen concentration and local overpotential. Local overpotential could be higher, but oxygen concentration must be lower under the shoulder. Since the dimension of the channel and shoulder are typically 0.5–2 mm the additional electron conduction path is only 0.25–1 mm. Would it be possible for such a short additional path along the GDL to cause enough additional ohmic loss to alter the current distribution? Zhou and Liu [29] presented modeling results that incorporates the anisotropic nature of the GDL electrical resistance. Instead of treating the GDL as isotropic, the fact that most currently used GDL materials have a much higher lateral conductivity was taken into consideration. Electron transfer in the catalyst layer was also taken into consideration. The results showed that when using realistic through-plane and in-plane GDL conductivities, the effect of GDL lateral electrical resistance was not large enough to cause the current density under the shoulder to be higher than that under the channel under any realistic operating conditions.

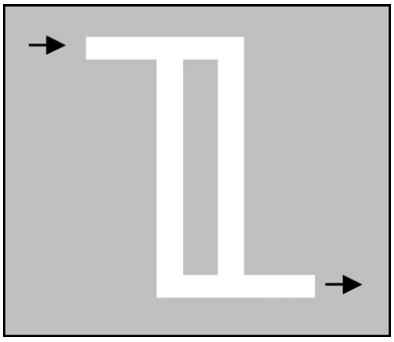

Fig. 2. Schematic of the cathode collector plate. White: machined channels.

Facing the contradicting modeling results, it is of great significance both academically and practically to know for sure where, under the shoulder or the channel, the current density is higher in a typical fuel cell, as well as the factors that affect the lateral current density distribution. Thus, the objectives of this study are to directly measure the current density under the channel and under the shoulder separately to determine where the current density is higher, to measure how large the difference is, and to determine the causes for the lateral current density variations.

2. Experimental methodology

In order to directly measure the current generated under the shoulder and under the channel, we must be able to electrically isolate the area under the shoulder from that under the channel. Since these two areas are electrically connected by a conductive GDL and catalyst layer, separate measurement of current is not possible with a regular fuel cell. Thus in order to achieve the objectives, specially designed fuel cells and MEAs were fabricated so that in each experiment either the current density under channel or under the shoulder could be measured alone.

The special fuel cell has a regular anode side with the full active area loaded with catalyst. The cathode flow field has only two parallel channels with a shoulder in the middle as shown as in Fig. 2. The width of the channels and shoulders are both 2 mm. In each set, three pieces of membrane electrode assembly (MEA) with different areas loaded with catalyst distribution were fabricated. One of them was loaded with catalyst only under the two channels as shown in Fig. 3(a). This arrangement was used to measure the current produced in the area under the channels. For this MEA, the "catalyst layer" under the shoulder had the same composition as that under the channels, except that there was no catalyst loading. The second MEA had catalyst loading only under the shoulder as shown in Fig. 3(b), with which the current produced under the shoulder was measured. Similarly, for this MEA the "catalyst layer" under the channels had the same composition, but without the catalyst. For both MEAs, the whole "catalyst layer" had the same thickness and the only difference at different areas was with or without catalyst loadings. The last MEA contained catalyst loading under both the channels and the shoulder as shown in Fig. 3(c), which was used to measure the total current produced by the PEM fuel cell. The gas diffusion layer is made of carbon cloth with a micro-diffusion layer.

A series of experiments with four different fuel cell pressures of 1, 1.68, 2.36 and 3 atm were conducted using three different MEAs, respectively. The cell temperature, humidification temperatures of the anode and cathode sides of the fuel cells were maintained at 70 °C. The flow rates of hydrogen and oxygen were 500 and 2000 sccm, respectively. The flow rates were set high to ensure stable operation of the fuel cell and to minimize the effect of the anode side.

The membrane used in the fuel cell was Nafion® 117 and was from Alfa-Aesar Company. The electrodes for the anode and cathode sides were provided by BCS Fuel Cell Company, made with carbon cloth loaded with platinum catalyst. The catalyst loading was 0.4 mg cm^{-2}. The area of the anode electrode was 50 cm^2, large enough to avoid any anode side boundary or local effects on the current density distribution. The total area of the cathode electrode was 3.36 cm^2. The membrane of and the electrodes for the anode and cathode sides were hot-pressed together under the temperature of 120 °C and pressure of 110 lbs cm^{-2}.

In order to determine if the GDL lateral resistance has a significant effect on the current density under the channel, a silver mesh was added between the collector plate and the GDL in the fuel cell with catalyst loading under the channels. The hypothesis that the GDL lateral electrical resistance caused the lower current density under the channel was based on the fact that for cathode reactions under the channel, electrons from the shoulder of the collector plate must first transfer laterally through the GDL to reach the catalyst layer under the channel. This additional electronic path incurs additional ohmic loss for the area

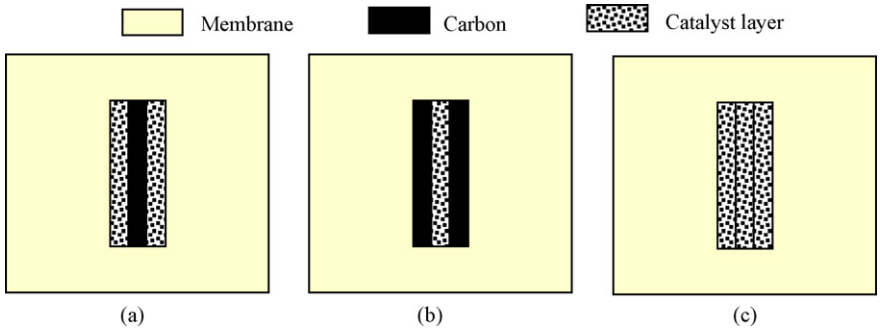

Fig. 3. A set of MEAs for separately measurement of current density under the channel and the shoulder. (a) MEA with catalyst under the two channels only, (b) MEA with catalyst under the shoulder only and (c) MEA with catalyst under both channels and the shoulder.

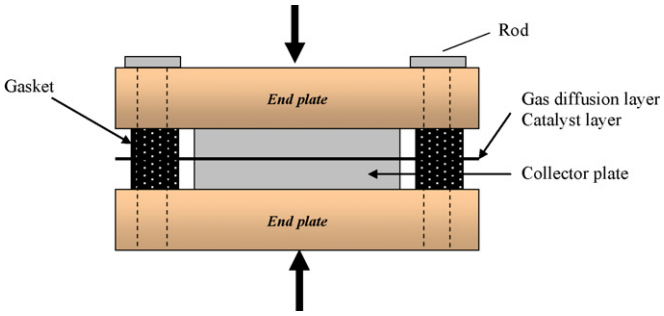

Fig. 4. The schematic of the test cell for the measurement of the through-plane electric resistance under different compressions.

under the channel. Though this additional ohmic loss does not have a significant effect on the cell voltage, it might have a significant effect on the local current density since the current density depends on overpotential exponentially. A slight change in local overpotential may cause a significant change in local current density, and it could be so significant that it could be more than compensate for the higher oxygen concentration under the channel. Due to the extremely high conductivity of silver mesh, if the GDL lateral electrical resistance is indeed the cause of lower current density under the channel, adding the silver mesh the performance of the fuel cell should improve significantly. The cell performance with this fuel cell was also tested under four different pressures, 1, 1.68, 2.36 and 3 atm.

To determine if the through-plane electrical resistance of the electrode is the cause for the lower current density under the channel, the total electrical resistance of the electrode (GDL with catalyst layer) was measured under different compressions. The experimental data will provide a reference of the difference between the total through-plane electric resistance of the gas diffusion layer and the catalyst layer under the channel and under the shoulder. The schematic of the test cell for the measurement of the through-plane electric resistance under different compressions is shown in Fig. 4. In the experiment, electrical resistance of the electrode was measured under different compressions and the amounts of compression were controlled by tightening the eight tie rods of the end plates. The torque applied to the tie rods was used as the reference for proper amount of compression and the distance between the end plates was measured to provide the amount of compression.

3. Experimental results and discussion

3.1. Validation of the experimental methodology

In order to validate the experimental methodology, experiments were conducted for all three MEA's. The currents produced with the MEA-a and MEA-b were added together and compared with MEA-c (See Fig. 3). Comparison results with different fuel cell pressures are shown in Figs. 5–8. For all the sets, the sums of the currents from the two partially catalyzed MEAs agree very well with the current produced by the fully catalyzed MEA, except when the current is beyond 2.5 A. When the current density is very high, the demand for reactant transfer is

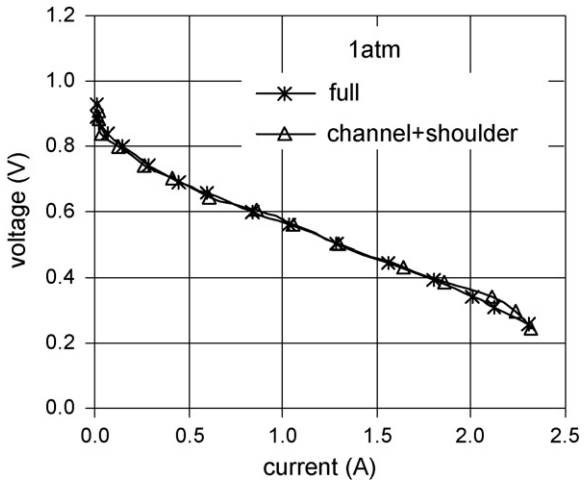

Fig. 5. Comparison of the current produced by the full-catalyzed cell with the total current produced by the two partially catalyzed cells. Anode humidification temperature = 70 °C; cathode humidification temperature = 70 °C; hydrogen flow rate = 500 sccm; air-flow rate = 2000 sccm; fuel cell pressure = 1 atm.

very high and the partially catalyzed case over-performs the full-catalyzed case since the latter has a larger area of reactant sink. Water generation rate may also play a roll in local mass transfer rate. Since the areas without catalyst have similar porosity as those with catalyst the difference in mass transfer rate is not significant under any practical operating conditions. These results validate the experimental methodology for separately measurement of currents under the channels and the shoulder of a PEM fuel cell.

3.2. Comparison of current density under the channel and the shoulder

With confidence in the methodology, the current densities under the channels are compared with that under the shoulder as shown in Figs. 9–12. It is obvious that the current density

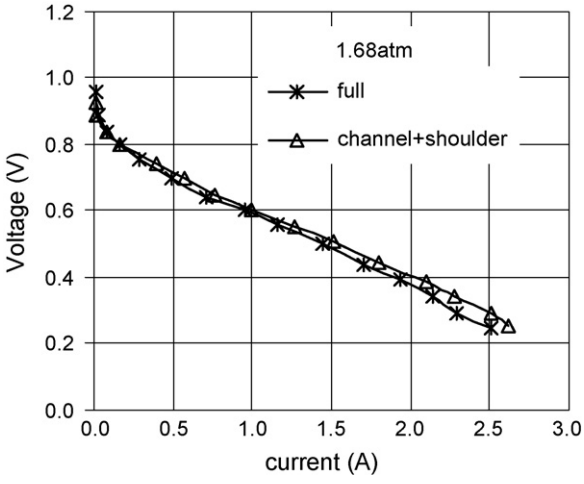

Fig. 6. Comparison of the current produced by the full-catalyzed cell with the total current produced by the two partially catalyzed cells. Anode humidification temperature = 70 °C; cathode humidification temperature = 70 °C; hydrogen flow rate = 500 sccm; air-flow rate = 2000 sccm; fuel cell pressure = 1.68 atm.

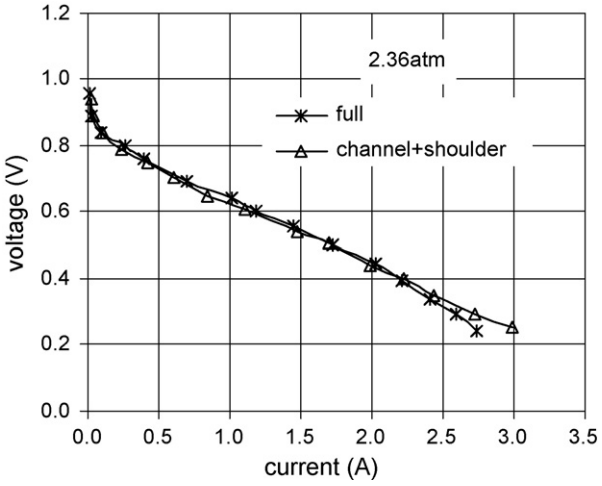

Fig. 7. Comparison of the current produced by the full-catalyzed cell with the total current produced by the two partially catalyzed cells. Anode humidification temperature = 70 °C; cathode humidification temperature = 70 °C; hydrogen flow rate = 500 sccm; air-flow rate = 2000 sccm; fuel cell pressure = 2.36 atm.

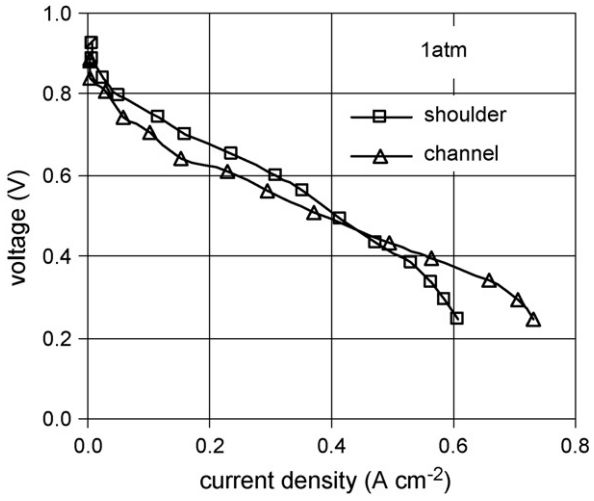

Fig. 9. Comparison between current density under the channel and the shoulder. Anode humidification temperature = 70 °C; cathode humidification temperature = 70 °C; hydrogen flow rate = 500 sccm; air-flow rate = 2000 sccm; fuel cell pressure = 1 atm.

under the shoulder is consistently higher than that density under the channel except in the high current density region. With the increase of the cell current density, the current density under the shoulder becomes lower than that under the channel. These results are clearly very different from those of earlier modeling results [22–25]. This phenomenon can be explained by the alternating dominant factors of mass transport and overpotential. In the low current density region, the difference in oxygen concentration between the areas under the channel and the shoulder is relatively small and the overpotential effect is dominant causing a higher current density under the shoulder. In the high current density region, due to the greater oxygen consumption rate, the difference in oxygen concentration between the areas under the channel and under the shoulder becomes so great that it becomes dominant and causes a higher current density under the channels. It is interesting to note from Figs. 9–12 that the crossing point, where the current densities from the two areas are equal, moves to higher current direction as the fuel cell operating pressure increases. At a higher pressure, oxygen mass transfer to the catalyst layer is enhanced and the effect of overpotential difference is more pronounced. It is possible for certain flow field design and operating conditions, either the current density under the shoulder or under the channel can be higher in the entire cell voltage range, but it is very clear from these experimental results that the difference in current densities in the two regions cannot be as great as predicted by the most of the models (e.g. [22–25]). The experimental results of this study are in very good qualitative agreement with the recent indirect measurement results [21].

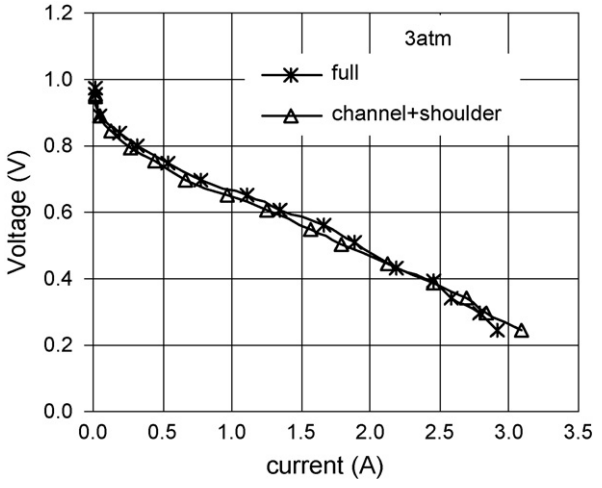

Fig. 8. Comparison of the current produced by the full catalyzed cell with the total current produced by the two partially catalyzed cells. Anode humidification temperature = 70 °C; cathode humidification temperature = 70 °C; hydrogen flow rate = 500 sccm; air-flow rate = 2000 sccm; fuel cell pressure = 3 atm.

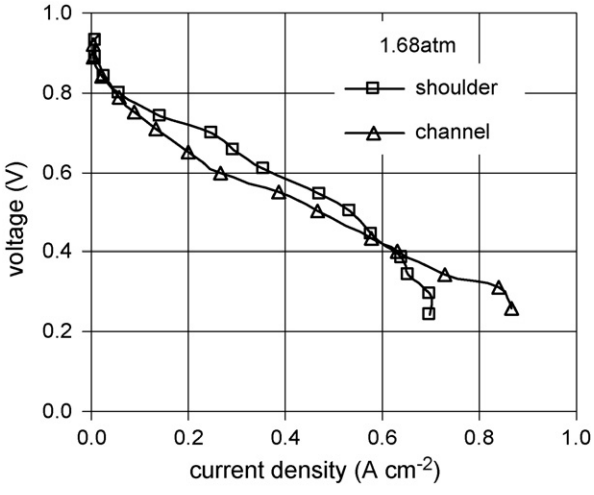

Fig. 10. Comparison between current density under the channel and the shoulder. Anode humidification temperature = 70 °C; cathode humidification temperature = 70 °C; hydrogen flow rate = 500 sccm; air-flow rate = 2000 sccm; fuel cell pressure = 1.68 atm.

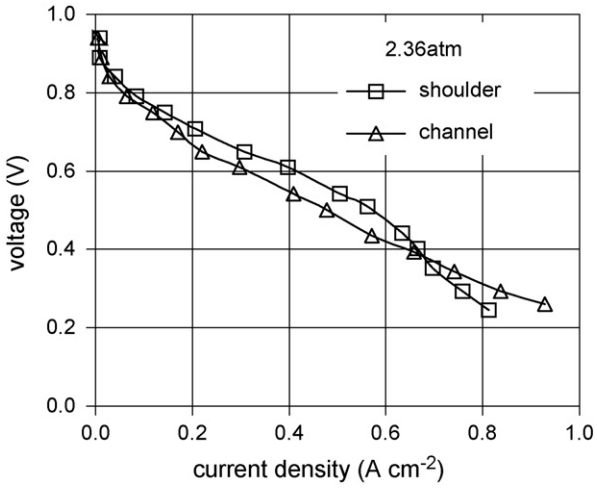

Fig. 11. Comparison between current density under the channel and the shoulder. Anode humidification temperature = 70 °C; cathode humidification temperature = 70 °C; hydrogen flow rate = 500 sccm; air-flow rate = 2000 sccm; fuel cell pressure = 2.36 atm.

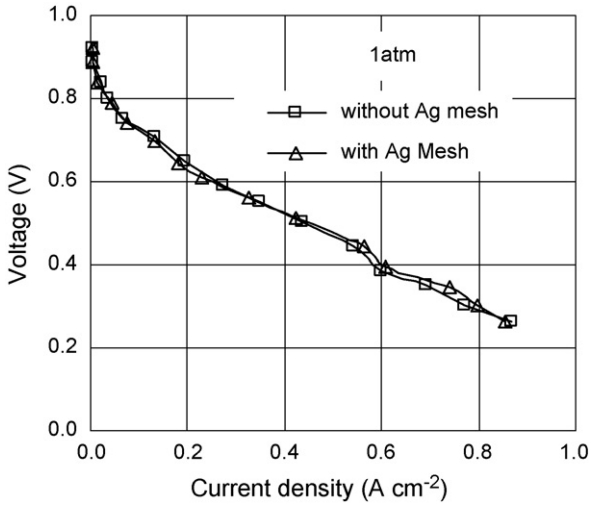

Fig. 13. Comparison of current densities with and without silver mesh under the channel. Anode humidification temperature = 70 °C; cathode humidification temperature = 70 °C; hydrogen flow rate = 500 sccm; air-flow rate = 2000 sccm; fuel cell pressure = 1 atm.

3.3. Effect of the GDL lateral electric resistance

Though direct measurement results showed the current density under the shoulder is indeed higher than that under the channel as predicted by some recent modeling works [26–28], it is still not clear if the GDL lateral electrical resistance is the cause as hypothesized [26–28]. To determine if the effect of the GDL lateral electrical resistance is the cause for higher current density under the shoulder, a series of experiments were conducted with the fuel cell with catalyst loading only under the channel. In these experiments, polarization curves for the cell under four different operating pressures were first obtained. Then the cell was disassembled and a silver mesh was added between the collector plate and the GDL. Another set of polarization were obtained from this cell with silver mesh. The polarization curves with and without the silver mesh under four different operating pressures of 1, 1.68, 2.36 and 3 atm, are compared and displayed in Figs. 13–16. It is obvious that the fuel cell performance did not show significant improvement by adding the silver mesh. To ensure that the process of dissembling the cell for adding the silver mesh would not alter the cell performance, the cell was tested again with the silver mesh removed. The cell performances were found identical with to those before adding the silver mesh. If the GDL lateral electrical resistance was the cause for the lower current density under the channel, adding the silver mesh would cause a significant increase of the current density under the channel due to the very high electrical conductivity of the silver mesh, which will eliminate the effects of GDL lateral resistance. Considering the thickness and the percentage of pores, the total conductance of the silver mesh was determined to be 3–4 orders of magni-

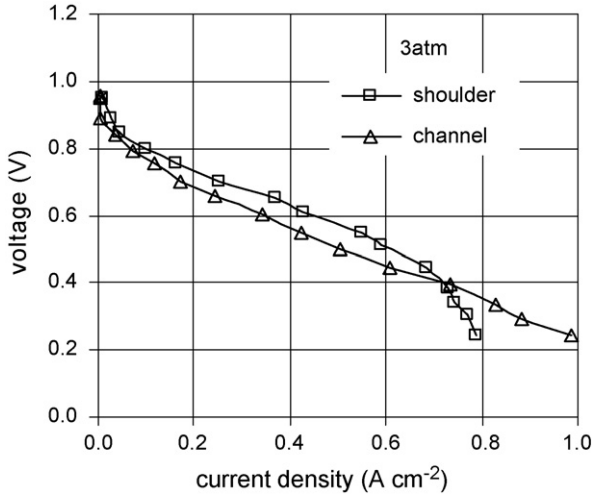

Fig. 12. Comparison between current density under the channel and the shoulder. Anode humidification temperature = 70 °C; cathode humidification temperature = 70 °C; hydrogen flow rate = 500 sccm; air-flow rate = 2000 sccm; fuel cell pressure = 3 atm.

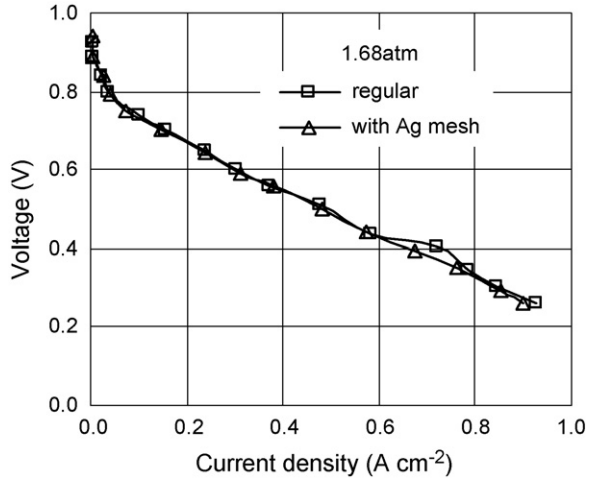

Fig. 14. Comparison of current densities with and without silver mesh under the channel. Anode humidification temperature = 70 °C; cathode humidification temperature = 70 °C; hydrogen flow rate = 500 sccm; air-flow rate = 2000 sccm; fuel cell pressure = 1.68 atm.

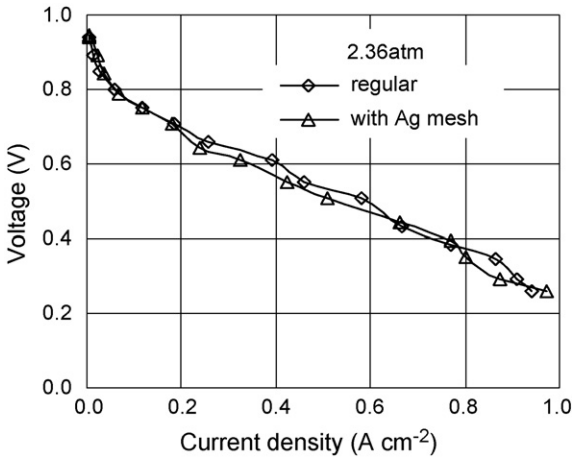

Fig. 15. Comparison of current densities with and without silver mesh under the channel. Anode humidification temperature = 70 °C; cathode humidification temperature = 70 °C; hydrogen flow rate = 500 sccm; air-flow rate = 2000 sccm; fuel cell pressure = 2.36 atm.

tude higher than that the GDL. Therefore it can be concluded from the unchanged cell performances that the lateral electric resistance not only is not the cause for the higher current density under the shoulder, but also has a negligible effect on the lateral current density distribution.

3.4. Effect of assembly compression under the shoulder

The experimental results showed that the current density was higher under the shoulder except in the high current region and it was found that the GDL lateral electrical resistance was not the cause. From the Bulter–Volmer equation (Eq. (1)) it can be seen that there are only two main differences between the area under the channel and that under the shoulder: local oxygen concentration and local overpotential. The local oxygen concentration under shoulder is definitely lower than that under the channel due to the longer diffusion path and the reduced porosity under compression. Thus the only factor that can cause the current density

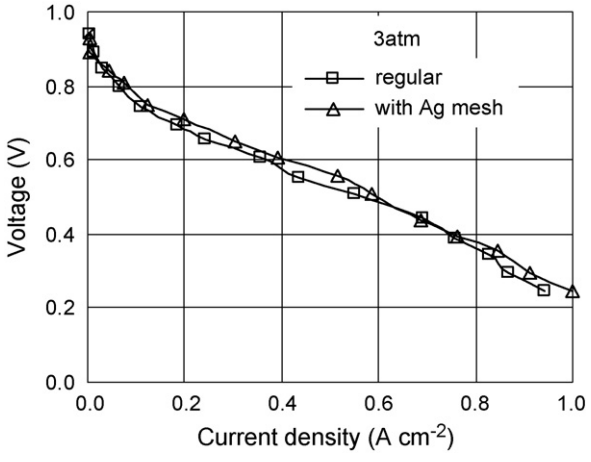

Fig. 16. Comparison of current densities with and without silver mesh under the channel. Anode humidification temperature = 70 °C; cathode humidification temperature = 70 °C; hydrogen flow rate = 500 sccm; air-flow rate = 2000 sccm; fuel cell pressure = 3 atm.

under the shoulder to be higher than, or even close to, that under the channel is a higher local overpotential. Yet it has been shown that the GDL lateral electrical resistance cannot be the cause of the higher local potential. The other factor that may cause a higher local overpotential is the lower total through-plane electric resistance under the shoulder due to assembly compressions. Therefore, the total through-plane electric resistance is measured under different compressions.

The results showed that under the compression corresponding to the amount under the shoulder in an operational fuel cell, the total though-plane resistance is only about 14% of the total value when the electrode was compressed by the weight of the collector plate plus the end plate and finger-tight of the tie rods. The difference in the through-plane electric resistance of the electrode between under the channel and under the shoulder could be so large that it is sufficient to cause the current density under the channel to be lower than that under the shoulder. It is understood that the measuring technique is not accurate and cannot differentiate the contribution of contact resistance and the through-plane resistance through the GDL and the catalyst layer. However, the results do indicate that the compression under the shoulder is the main contributor to the higher current density under the shoulder. After this work was submitted, the recent paper by Hottinen et al. [30] was brought to our attention. Interestingly enough, the general trend of their modeling results agree well with our direct measurement data.

4. Conclusions

A novel yet simple approach was employed to directly measure the current densities under the channel and the shoulder separately in PEM fuel cells with parallel flow field. In this approach, the cathode catalyst layer was designed to have either the area under the shoulder or the area under the channel loaded with catalyst. Such a design guaranteed the currents generated under the shoulder and the channel could be measured separately without any possible interference. From the experimental results, the following conclusions can be made for PEM fuel cells with parallel flow field and under well-humidified conditions:

- Local current density under the shoulder is higher than that under the channels except at the high current density region. This means the effect of higher local overpotential is large to overshadow the effect of lower oxygen concentrations.
- In the high current region, current density under the shoulder is lower than that under the channel, indicating the predominant effect of lower local oxygen concentrations.
- The effect of GDL lateral electrical resistance is not the cause for higher current density under the shoulders and it does not have a significant effect on lateral current density distributions.
- The higher current density under the shoulder could be caused by the increased conductance due to local compressions, though for different MEA's the effect of compression could vary.

References

[1] D. Brett, S. Atkins, N. Brandon, V. Vesovic, N. Vasileiadis, A. Kucernak, Electrochem. Commun. 3 (2001) 628.
[2] M.M. Mench, C.Y. Wang, M. Ishikawa, J. Electrochem. Soc. 150 (2003) A1052.
[3] D. Natarajan, T.V. Nguyen, J. Power Sources 135 (2004) 95.
[4] D. Natarajan, T.V. Nguyen, AIChE J. 51 (2005) 2587.
[5] D. Natarajan, T.V. Nguyen, AIChE J. 51 (2005) 2599.
[6] S.J. Cleghorn, C.R. Derouin, M.S. Wilson, S. Gotterfeld, J. Appl. Electrochem. 28 (1998) 663.
[7] J. Stumper, S.A. Campbell, D.P. Wilkinson, Electrochim. Acta 43 (1998) 3773.
[8] N. Rajalakshmi, M. Raja, K.S. Dhathathreyan, J. Power Sources 112 (2002) 331.
[9] Z. Liu, Z. Mao, B. Wu, L. Wang, V.M. Schmidt, J. Power Sources 141 (2005) 205.
[10] P.C. Ghosh, T. Wüster, H. Dohle, N. Kimiaie, J. Mergel, D. Stolten, J. Fuel Cell Sci. Technol. 3 (2006) 315.
[11] C. Wieser, A. Helmbold, E. Gulzow, J. Appl. Electrochem. 30 (2000) 803.
[12] F.N. Büchi, A.B. Geiger, R.P. Neto, J. Power Sources 145 (2005) 62.
[13] H. Sun, G. Zhang, L. Guo, H. Liu, J. Power Sources 158 (2006) 326.
[14] H. Sun, G. Zhang, L. Guo, D. Shang, H. Liu, J. Power Sources 168 (2007) 400–407.
[15] M. Noponen, T. Mennola, M. Mikkola, T. Hottinen, P. Lund, J. Power Sources 106 (2002) 304.
[16] T. Hottinen, M. Noponen, T. Mennola, O. Himanen, M. Mikkola, P. Lund, J. Appl. Electrochem. 33 (2003) 265.
[17] D.G. Strickland, S. Litster, J.G. Santiago, J. Power Sources 174 (2007) 272–281.
[18] A. Hakenjos, H. Muenter, U. Wittstadt, C. Hebling, J. Power Sources 131 (2004) 213.
[19] A. Hakenjos, C. Hebling, J. Power Sources 145 (2005) 307.
[20] W.H.J. Hogarth, J. Steiner, J.B. Benziger, A. Hakenjos, J. Power Sources 164 (2007) 464.
[21] S.A. Freunberger, M. Reum, J. Evertz, A. Wokaun, f.N. Büchia, J. Electrochem. Soc. 153 (2006) A2158.
[22] T. Zhou, H. Liu, Int. J. Trans. Phenomena. 3 (2001) 177.
[23] T. Berning, D.M. Lu, N. Djilali, J. Power Sources 106 (2002) 284.
[24] U. Sukkee, C.Y. Wang, J. Power Sources 125 (2004) 40.
[25] D. Natarajan, T.V. Ngyuen, J. Electrochem. Soc. 148 (2001) A1324.
[26] H. Meng, C.Y. Wang, J. Electrochem. Soc. 151 (2004) A358.
[27] B.R. Sivertsen, N. Djilali, J. Power Sources 141 (2005) 65.
[28] G. Lin, T.V. Nguyen, J. Electrochem. Soc. 153 (2006) A372.
[29] T. Zhou, H. Liu, J. Power Sources 161 (2006) 444.
[30] T. Hottinen, O. Himanen, S. Karvonen, I. Nitta, J. Power Sources 171 (2007) 113.